Patch Clamp Techniques for the Characterization of Membrane Channels

R. Eckert, D. Paschke and D. F. Hülser

Division of Biophysics, Biological Institute, University Stuttgart

Membranes play a dominant role in processing and transferring information in biological systems. Well known examples are conductivity changes in membranes of excitable cells by which information transfer is mediated. The electrical phenomena at the nerve membrane are well documented since the pioneering experiments of Hodgkin et al. (1952) who demonstrated the movement of sodium and potassium ions across the membrane during action potentials. Using voltage clamp techniques and selective blockers, they succeeded in separating the currents carried by these two ions. Their results were best interpreted by assuming selective channels with variable conductivity which, however, could not be resolved at this time. Introducing the patch clamp technique, Neher and Sakmann (1976) stimulated membrane research by an electrophysiological method which led to the characterization of many membrane channels. With this technique minute changes of ionic permeability became detectable, leading to an understanding of the opening and closing behaviour of membrane channels and of the molecular mechanisms by which biological membranes maintain and modulate their permeability for specific ions.

A simple experimental setup for the determination of electrical properties of the cell membrane is depicted in Fig. 1. It uses a glass micropipette filled with 3 M KCl saline as an electrode and a voltage amplifier to measure the transmembrane potential of the impaled cell against an indifferent electrode located in the extracellular medium. With this setup, however, it is impossible to measure the quantities needed to determine membrane conductances, which serve as an index for ionic permeability. Using only a single electrode, current and voltage cannot be measured simultaneously. Because of the resistance of the microelectrode in series with the input resistance of the cell, conceivable errors in the voltage measurement will occur when current is injected and vice versa.

The classical setup for studying membrane currents or membrane resistances is the voltage clamp technique used by Hodgkin et al. (1952). This setup (Fig. 2) uses two separate microelectrodes for current and voltage determination in order to avoid any distortions from the electrode resistances. The microelectrodes are connected to each other via an operational amplifier. This amplifier determines the transmembrane potential by the voltage electrode and keeps it at a preset constant value (the holding potential, U_{Hold}) by regulating the current through the current electrode. A holding potential can be applied to the input of the operational amplifier which serves as the reference for the voltage determination. Control of transmembrane voltages and the measurement of the respective currents allow a continuous determination of membrane conductances over a wide range of experimental conditions. The impalement of a cell with a glass microelectrode, however, causes a

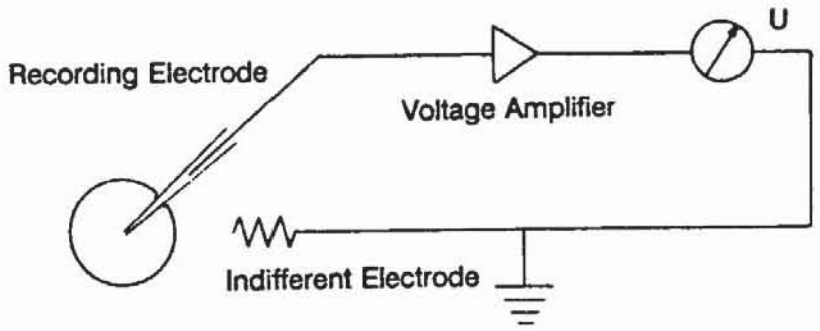

Fig. 1: Experimental setup for intracellular recording of membrane potentials with a glass microelectrode.

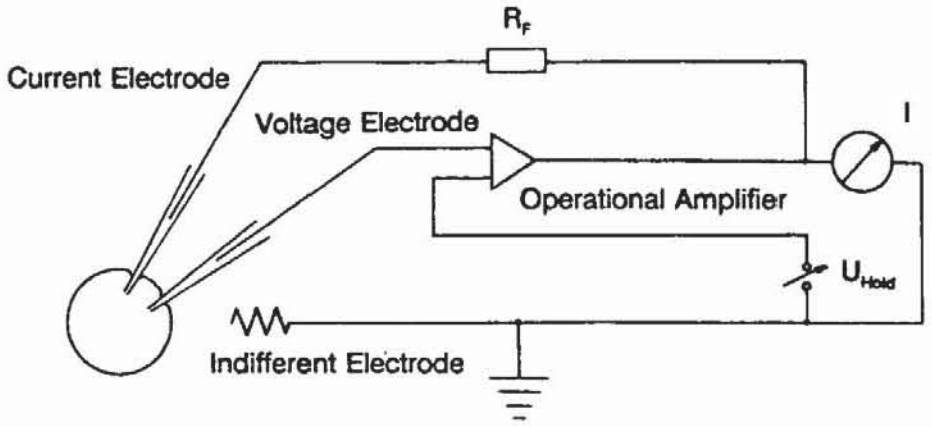

Fig. 2: Electrical setup of voltage clamp experiments using two microelectrodes.

substantial shunt resistance in parallel to the membrane resistance (Fig. 3). This shunt resistance is often in the order of, or smaller than the cell membrane resistance and, therefore, will be the main source of noise in this kind of setup, where two electrodes must be inserted. Thus, the upper limit of the current resolution will be determined mainly by this "seal" resistance and the signal to noise ratio becomes too low for the resolution of single molecular events; an average behaviour for the bulk population of the membrane channels is measured instead.

With the patch clamp technique (Neher & Sakmann, 1976 and Hamill et al., 1981), however,

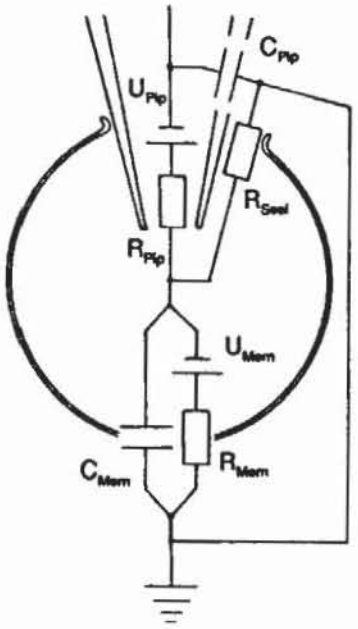

Fig. 3: Equivalent circuit for intracellular recording with conventional glass microelectrodes.
U_{Pip} = pipette potential
C_{Pip} = pipette capacitance
U_{Mem} = membrane potential
C_{Mem} = membrane capacitance
R_{Pip} = pipette resistance
R_{Seal} = seal resistance
R_{Mem} = membrane resistance

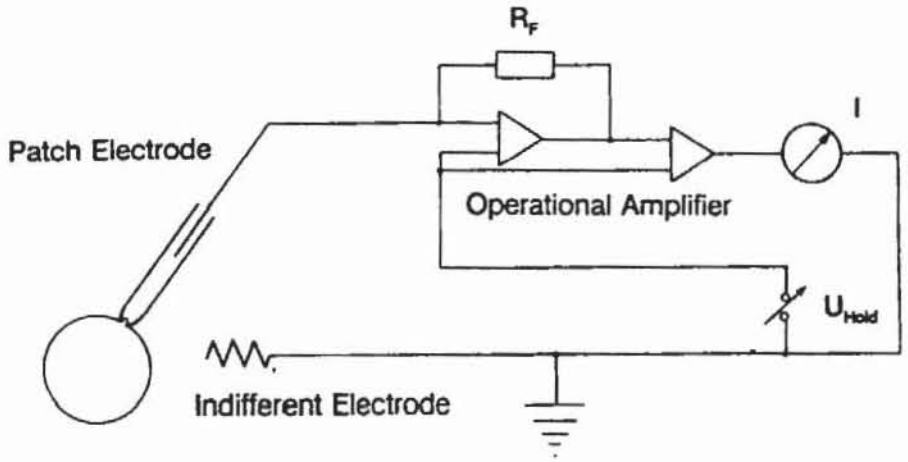

Fig. 4: Electrical setup of patch clamp experiments (redrawn from Sigworth, 1983).
U_{Hold} = Holding potential
R_F = Feedback resistor

the electrical characterization of individual channels is no longer a problem. It is - in essence - a modification of the voltage clamp technique (compare Fig. 4 and Fig. 2) with special arrangements to improve the sealing of the glass microelectrode to the cell

membrane. Special microelectrodes (patch-type or suction electrodes) are used, which are pressed against the cell surface rather than inserted into the cell. Thus, only a small membrane area under the tip of the electrode (the "patch") is used for current measurements. This results in a totally different situation with respect to resistances than is found with whole cell voltage clamp experiments. The seal resistance increases by two orders of magnitude to the range of several GΩ ("Gigaseals") and is similar to the resistance of the patch membrane, while the access resistance of the pipette is usually much lower (about 1 - 10 MΩ) compared to standard microelectrodes. In addition, the small membrane patch reduces the number of active channels to a level, where the contribution of a single channel to the total membrane current becomes discernible. With the improved sealing properties of patch-type pipettes it is possible to record current and voltage through a single electrode and, thus, artifacts originating from the impalement of the cell membrane by microelectrodes are further reduced. The total resistance of the cell membrane outside the patch is very low compared to that of the patch, while the currents flowing through the patch are usually small (some pA). The patched membrane may, therefore, be regarded as locally voltage clamped by one electrode. Furthermore, the mechanical stability of the seal offers the opportunity to isolate the patch from the cell and measure in a cell-free system where all parameters are determined solely by the experimenter.
In this contribution we will discuss not only the prerequisites necessary to perform patch clamp experiments, but also the analysis and interpretation of the resulting data.

Glass microelectrodes

Glass microelectrodes have always been an essential tool in electrophysiological measurements, and this is especially true for the patch clamp technique. One of the most striking modifications from voltage clamp to patch clamp measurements concerns the totally different shape of the glass micropipettes used for the electrodes. Conventional glass micropipettes are designed for impalement of the cell, i.e. they are formed like a sharp needle with a very small tip diameter (0.1 μm). In contrast, patch pipettes are blunt, with steeply tapered tips and opening diameters of 0.1 - 1 μm. They are pulled using a two step procedure which leads to their typical shape (Fig. 5).
The raw material used for the fabrication of pipettes are capillaries (outer diameter 1 - 2 mm) either from soft glass (soda lime glass) or hard glass (usually borosilicate or quartz glass) without an inner filament (but see Burt & Spray, 1988). Soft glass is easy to handle but lacks somewhat the insulating properties of hard glass. This can be compensated partially by coating the pipette tip with hydrophobic materials such as beeswax or Sylgard™, a silicone resin which reduces the noise levels considerably. Since the mechanisms of membrane to glass interactions which form the seal are not completely known (Corey & Stevens, 1983), no general advice can be given for choosing the right glass material for any specific task. Hard glass seems to have better sealing properties with artificial membranes than soft glass (Corey & Stevens, 1983) and was also recommended for some primary cell

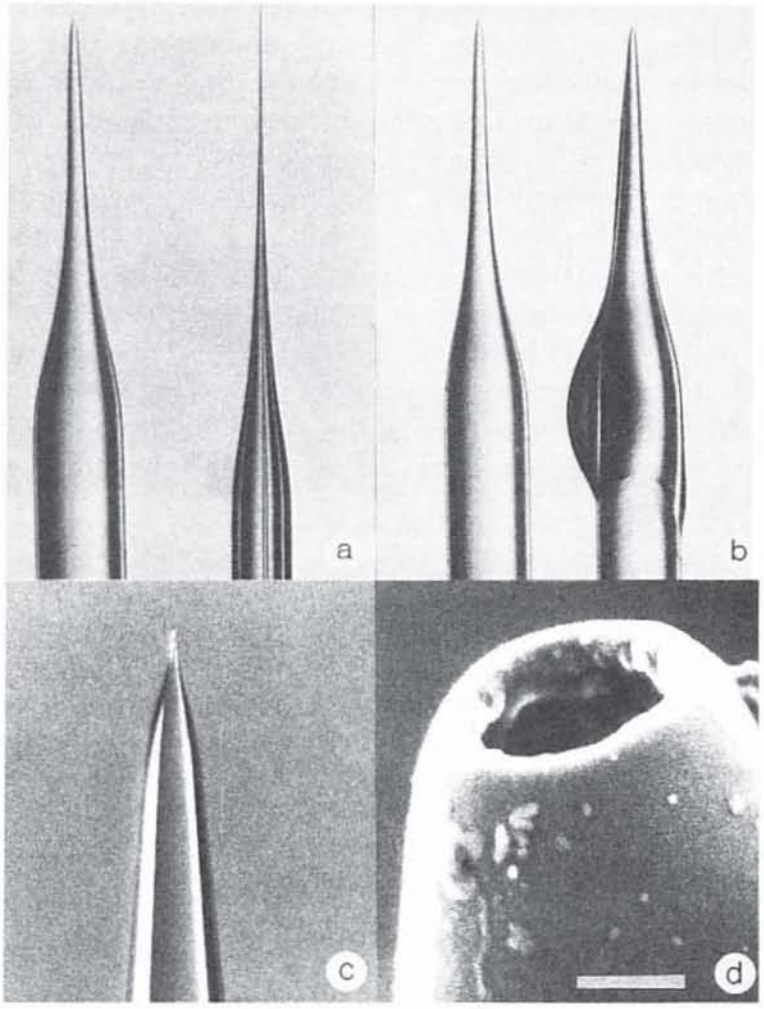

Fig. 5: a. Comparison of the shape of a conventional glass micropipette (right) with a patch-type pipette (left).
b. Sylgard coated (right) and uncoated (left) patch pipette.
c. Shape of a patch pipette tip; note the steep taper originating from the two step pulling procedure.
d. Scanning electron micrograph of the immediate tip of a polished soft glass pipette (bar: 200 nm).

lines (Rae & Lewis, 1984; Cota & Armstrong, 1988). In our hands, pipettes made from soft glass (CeeBee hematocrit capillaries, o.d. 1.5mm - Chr. Bardram, Svendborg, Denmark) yield good results both with primary and with permanently growing cells.
As mentioned before, patch pipettes are pulled in two steps in order to form the typical steep tapered tip shape. During the first pull a high heating current is applied to create an appropriate wall thickness of the capillaries for the second step. After the pipette is recentered, the second pull is carried out with lower heating current. This is a critical step because the heating determines the final geometrical parameters of the tip, such as shank and tip diameter. Tip diameters of soft glass electrodes are usually in the range of 1 μm corresponding to an input resistance of 4-10 MΩ when filled with 140 mM KCl (Sakmann & Neher, 1983).

After pulling, the pipette rawlings usually are coated with hydrophobic materials such as Sylgard™ (Dow Corning Inc., Seneffe, Belgium) or beeswax (Fig. 5b). This coating is necessary to improve the capacitive properties of the glass cylinder and its adhering fluid film which act as a stray capacitor in parallel to the input resistance of the electrode. With pipettes made from soft glass, coating also reduces current leakage of ions passing the swollen glass (Corey & Stevens, 1983). This results in a substantial decrease of the background noise level and enables recording with high input resistances.
The next step towards suitable patch pipettes is heat polishing of the pipette tip. This procedure creates a smooth rounded rim at the tip where the pipettes were broken apart during the second pull and also burns off the thin sylgard film covering the pipette tip. Polishing is performed under microscopical control by pushing the pipette tip close to a red glowing platinum wire until the white (sharp) rim at the tip changes to a smooth black line. Polishing also affects tip geometry and may be used, therefore, to reduce the pipette input resistance to a certain degree.

Pipette filling

Due to the large tip diameter of the pipette facing the patch or - with whole cell recordings - the cell interior, patch electrodes may not be filled with the 3 M KCl solutions commonly used for conventional microelectrodes. The ionic compounds of the pipette solution should match as closely as possible those of the medium to which the membrane is normally exposed. For cell attached and inside out patches extracellular solutions are used as pipette filling whereas for outside out patches and whole cell recordings intracellular compounds are appropriate. In Table 1 several pipette solutions are listed which may be used with mammalian cells.
Prior to use, all solutions must be filtered through a 0.2 μm membrane filter (nitrocellulose or nylon) to prevent clogging of the pipette tip with particles or any contamination (e.g. from protein) which may interfere with the formation of a gigaseal.

Pipette holders

Pipette holders for patch pipettes are designed for pressure application to the filling solution (Fig. 6). For a detailed description of the mechanical setup of a pipette holder see Hamill et al. (1981). In addition, other requirements may be requested such as rapid solution exchange in the pipette tip which may result in a somewhat altered design of the pipette holders (e.g. Cull-Candy & Parker, 1983; Lapointe & Szabo, 1987). A silver wire coated with AgCl which is inserted into the pipette shaft is used as a non polarizing electrode.

Table 1 Solutions Used for Patch Clamp Experiments

Extracellular salines	
$E_{1.4}$:	140 mM NaCl, 5 mM KCl, 1.4 mM $CaCl_2$, 0.5 mM $MgCl_2$, 10 mM HEPES/NaOH (pH 7.3).
E_{gluc} :	110 mM NaCl, 5 mM KCl, 0.5 mM $CaCl_2$, 0.5 mM $MgCl_2$, 10 mM glucose, 10 mM HEPES/NaOH (pH 7.3).
Intracellular salines	
I_{140} :	140 mM KCl, 0.01 mM $CaCl_2$, 1 mM $MgCl_2$, 5 mM EGTA/KOH, 10 mM HEPES/KOH (pH 7.3).
I_{140} - low calcium:	140 mM KCl, 5 mM EGTA/KOH, 10 mM HEPES/KOH (pCa $>$ 7, pH 7.3).
I_{ATP}- ATP+cAMP:	140 mM KCl, 5 mM EGTA/KOH, 5 mM K_2ATP, 0.1 mM Na db-cAMP, 10 mM HEPES/KOH (pH 7.3).
I_{asp} - aspartate :	120 mM K aspartate, 5 mM EGTA/KOH, 10 mM HEPES/KOH (pH 7.3).

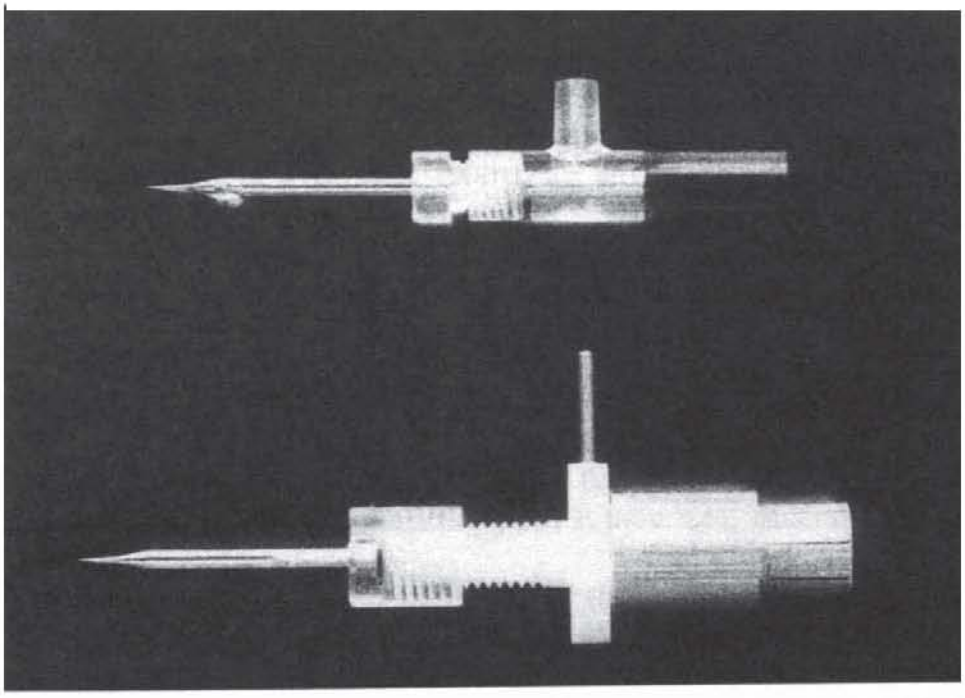

Examples of pipette holders appropriate for patch clamp experiments. Note the inlet for pressure application.

Electronic and mechanical setup for patch clamp measurements

The principle electronic setup for patch clamp measurements is depicted in Fig. 4 (for a detailed discussion see Sigworth, 1983). Our experiments were performed with List EPC-7 patch clamp amplifiers (List Electronic, Darmstadt, FRG) where appropriate filters are provided within the amplifier. The current signals observed with the patch clamp amplifier usually must be filtered with analog filtering devices to improve the signal to noise ratio. The signal is then displayed on a high resolution digital storage oscilloscope (e.g. Nicolet 3091) for first inspection of the data records. Digital storage oscilloscopes are convenient for this task because most of them provide a "roll off" mode for display and cursors for a crude data analysis. Data may be stored permanently on a tape recorder or on video tape (Bezanilla, 1985) via a digital audio processor (e.g. Sony PCM-501ES) to provide high fidelity and sufficient frequency bandwidth. The stored records may later be played back and digitized for a subsequent analysis with a microcomputer. Inexpensive microcomputers with high speed and large storage capacity equipped with appropriate A/D-D/A converters with high data throughput may be used directly for experimental control (e.g. complex voltage pulse programs) and data storage (see McCann et al., 1987). A waveform generator connected to the stimulus input of the amplifier serves as an external voltage source for the application of command pulses and determination of electrode resistances. To minimize noise from external sources the whole setup is enclosed in a Faraday cage.
During patch clamp measurements even minute vibrations may affect the stability of the patch, therefore, the experiments must be performed on a shock absorbing table with heavy weights. For the observation of the cells and the positioning of the electrodes an inverted microscope with phase contrast equipment is appropriate. The headstage of the amplifier with the pipette holder is mounted on electrically or mechanically driven micromanipulators which allow the fine movements of the electrodes necessary to perform patch clamp experiments.

The patch clamp procedure

Patch clamp experiments require cells with a "smooth" membrane when a high ohmic sealing should be established. In our hands, with cultured mammalian cells this is best achieved by a short treatment with 2.5% trypsin 30 - 60 min prior to the experiments. With biopsies of primary cells such a proteinase treatment is usually included in the preparation procedure (Bräuner, 1987).
A typical patch clamp experiment proceeds like this: The pipette is inserted into the holder and a positive pressure of about 100 mm H_2O is applied to its interior. After the tip passes the air/water interface of the bath medium, this pressure results in an outflux of pipette medium which should prevent contamination of the sealing area of the tip (Fig. 7-1). The input resistance is monitored continuously by application of rectangular voltage pulses with fixed amplitude (10 mV) and determination of the resulting current output on an

oscilloscope. Changes in the current output reflect changes in electrode resistance. Under microscopical control, the electrode is manipulated close to the cell surface until it just touches the cell membrane (Fig. 7-2). Now the pressure is released from the pipette interior and usually a twofold increase of the input resistance will be observed, sometimes even a gigaseal is already achieved at this step of the procedure.

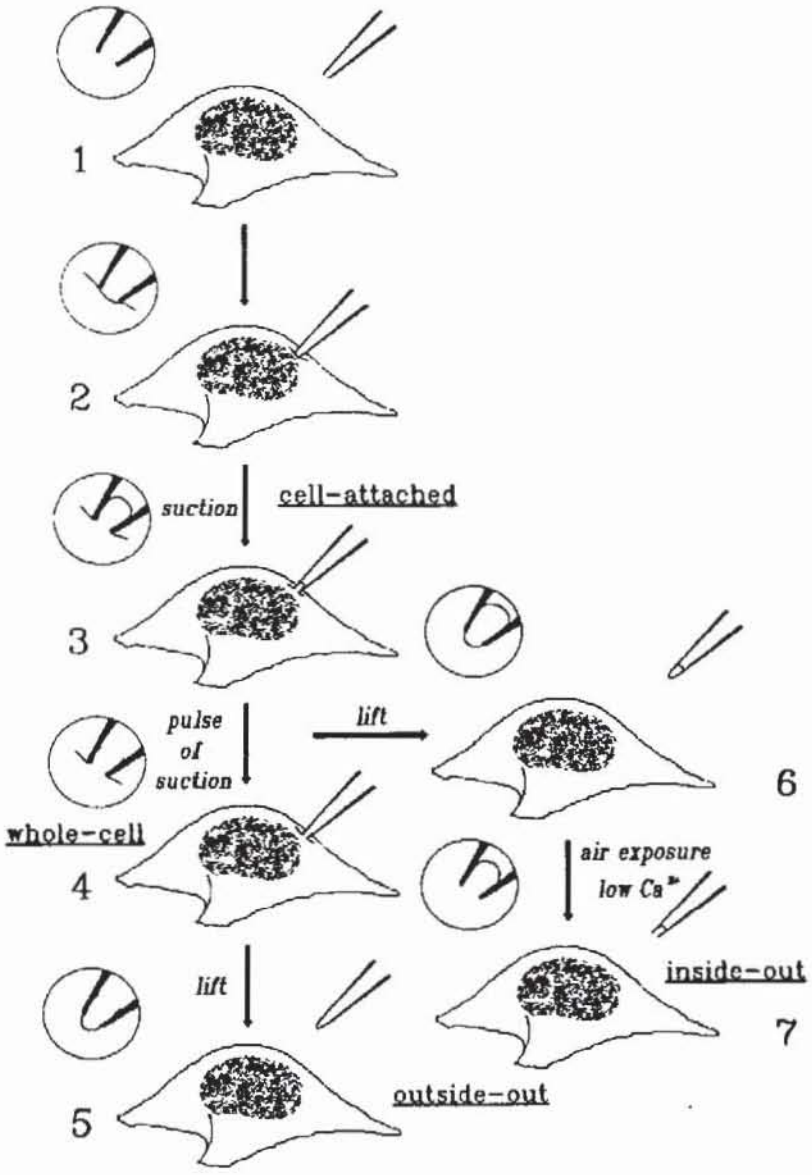

Fig. 7: A short outline of patch clamp procedures. For detailed description see text.

Cell attached configuration

A short pulse of suction (best applied by mouth) pulls an Ω-shaped piece of membrane into the pipette tip and the gigaseal may form (Fig 7-3). This can easily be seen from the diminishing current signal indicating a considerable increase of the input resistance. With this step the basic mode of the patch clamp procedure called "cell attached" or "on cell" mode is established. The patch of membrane in the pipette tip is connected to the rest of the cell via the cytoplasm, however, because of the gigaseal it is electrically isolated from the remainder of the cell membrane. Thus, while the membrane resistance is about one order of magnitude lower than the patch resistance, the patch itself may be regarded as locally voltage clamped by the voltage setting of the patch electrode (Fig. 8). This configuration is especially suitable when intracellular mechanisms are suspected to influence the process under study. The gating behaviour of many ion channels is modulated or evoked via cyclic nucleotides or divalent cations such as Ca^{2+} or Mg^{2+}, e.g. the effects of serotonin in Aplysia neurons are mediated by cAMP as a second messenger (Camardo & Siegelbaum, 1983).

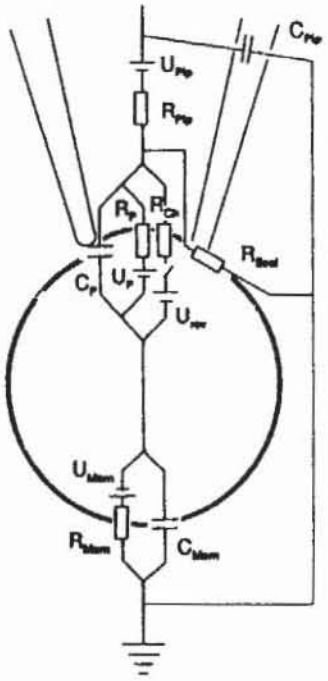

Fig. 8: Equivalent circuit for the cell attached patch clamp configuration.

U_{Pip}	=	pipette potential	R_{Pip}	=	pipette resistance
C_{Pip}	=	pipette capacitance	U_P	=	patch potential
R_P	=	patch resistance	C_P	=	patch capacitance
U_{Mem}	=	membrane potential	R_{Mem}	=	membrane resistance
C_{Mem}	=	membrane capacitance	R_{Seal}	=	seal resistance
U_{rev}	=	reversal potential	R_{Ch}	=	open channel resistance

The cell attached configuration probably causes less deviation from the natural conditions than any other method for membrane resistance measurement (and certainly than any other patch mode). The disadvantage of this method, however, is the lack of a direct measurement of the voltage difference across the patch because the transmembrane potential - which is in series with the holding potential - is usually not accessible while performing such measurements. Unfortunately, it may be impossible to rupture the patch membrane at the end of a long-lasting experiment so that the transmembrane potential cannot be determined for these measurements. Furthermore, the composition of the cytosol cannot be controlled in this configuration. The pipette solution, however, may be exchanged, but no simple method is available for changing media inside a patch pipette. Pipette perfusion has been described for different systems where tubings are inserted into the patch pipette (Cull-Candy & Parker, 1983; Lapointe & Szabo, 1987) but these perfusion setups are difficult to manipulate and hard to control.

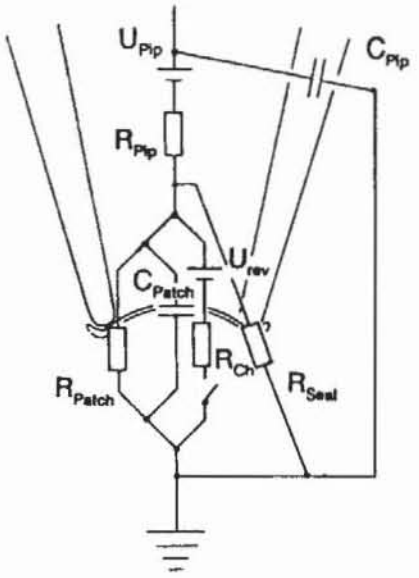

Fig. 9: Equivalent circuit for the cell free patch modes inside-out and outside-out.

U_{Pip}	=	pipette potential	R_{Pip}	=	pipette resistance
C_{Pip}	=	pipette capacitance	R_{Seal}	=	seal resistance
R_{Patch}	=	patch resistance	C_{Patch}	=	patch capacitance
U_{rev}	=	reversal potential	R_{Ch}	=	open channel resistance

Inside-out and outside-out configuration

Easy access to at least one side of the patch solution is possible when one of the cell free modes is used: either "outside-out" (Fig. 7-5) or "inside-out" (Fig. 7-7) patches, where one side of the patched membrane faces the bath medium. Because the bath medium is

exchanged rapidly using relatively simple setups, cell free membrane patches are ideally suited to study transmitter evoked channel activity, ion selectivity, and a multitude of other questions. Since no other cell membrane is in series to the patch (Fig. 9), cell free patches are directly voltage clamped and the apparent holding potential equals the voltage difference across the patch. This gives the experimenter a sufficient control over a wide variety of experimental conditions and it explains the widespread use of cell free configurations throughout the literature.
An inside-out patch is obtained after pulling off the pipette from the cell attached configuration (Fig. 7-6). In most cases the result will be a small membrane vesicle at the pipette tip. Vesicles have a larger capacitance compared to the cell attached and inside-out patches and may be identified by their large capacitive transients when square pulses are applied. When the pipette is lifted out of the bath medium and exposed to air, the outer part of the vesicle will break and the inside-out patch configuration is obtained (Fig. 7-7). It is called "inside-out" because the inner or cytoplasmic membrane surface is exposed to the bath medium, which is considered to be "outside". In media with low contents of free Ca^{2+}, vesicle formation often fails and the inside-out patch is reached directly.
Establishing an outside-out patch is achieved analogously by first rupturing the cell membrane and then pulling a "half vesicle" from the cell membrane (Fig. 7-5). This is also called a "right-side-out" patch because now the extracellular surface faces the "extracellular" bath medium while the pipette medium is considered to represent the cytoplasmic composition. The advantage of cell free membrane recordings is somewhat diminished by the fact that cell free membrane patches become artificial systems which lack most of the biological regulatives normally present in the intact cell. For some questions this can be an advantage, it may, however, also lead to severe misinterpretation of the measured data.

Whole cell recording

When disrupting the patch membrane for the outside-out patch the fourth mode of the patch clamp is reached (Fig. 7-4), where the terminus "patch" clamp does not really apply to because there is no membrane patch involved. This is, therefore, called "tight seal whole cell recording" (Marty & Neher, 1983). Whole cell recording with patch pipettes is an alternative to the conventional voltage clamp techniques, when applied to small cells as are often found in permanently growing mammalian cell lines. Small cells are not adequate for standard voltage clamp procedures due to cell damage caused by the insertion of two microelectrodes. Impalement introduces a shunt resistance which often decreases the input resistance of the cell to about a half of its normal value and reduces the signal to noise ratio to unacceptable levels. Whole cell recording damages the cell membrane to a minor degree and results in far better seals. Its application, however, is restricted to small cells only, with diameters of about 10μm - or in terms of electrical properties - with input resistances of about 100 MΩ or more. The restriction originates from the fact, that a single electrode is used for current and voltage determination (Fig. 10) where the series resistance cannot be

neglected and, therefore, should be less than 1% of the total input resistance of the system. Due to the wide opening diameter of patch pipettes a conceivable exchange of the pipette solution with the cytosol as well as a diffusion of higher molecular components into the pipette will occur (Marty & Neher, 1983; Pusch & Neher, 1988). This offers the possibility of rapid internal perfusion of cells with defined media (Kostyuk et al., 1981), a "dialysis" of the cell interior against the pipette filling which often causes inhomogeneities during the recording interval. Pipette media for whole cell recordings, therefore, are often supplemented with additional components such as glucose, aspartate, glutamate (in exchange for Cl^-), or even ATP and cAMP to reduce this uncontrolled dialysis (Somogyi & Kolb, 1988, Paschke, 1989). On the other hand, dialysis can be prevented by permeabilizing the membrane of cell attached patches to such a degree that a high ionic current is facilitated. With such a reduced access resistance, this mode corresponds to whole cell recording. A recent approach uses nystatin - an antibiotic which formes cation selective channels in the membrane - as mediator between cell- and pipette-interior to study the activation of muscarinic currents in rat lacrimal gland cells (Horn & Marty, 1988).
Thus, whole cell recording may be considered as an additional procedure for voltage clamp studies of small cells, which - within the limitations of the method - offers several advantages opposed to conventional techniques.

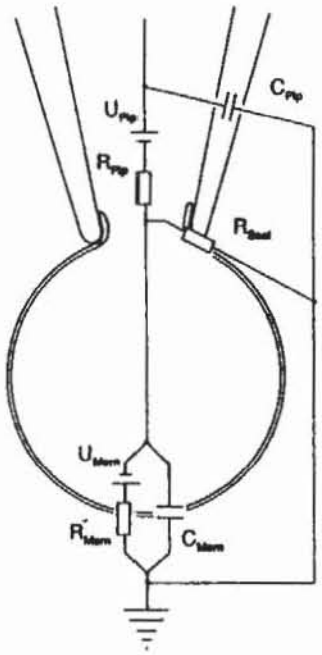

Fig. 10: Equivalent circuit for tight seal whole cell recording with patch electrodes.

U_{Pip}	= pipette potential	R_{Pip}	= pipette resistance
C_{Pip}	= pipette capacitance	R_{Seal}	= seal resistance
U_{Mem}	= membrane potential	R_{Mem}	= membrane resistance
C_{Mem}	= membrane capacitance		

Double whole cell recording for the characterization of gap junction channels

A derivative of this procedure - the double whole cell recording technique - has been developed by Neyton & Trautman (1985) to study the properties of a channel species which mediates between the cytoplasm of two adjacent cells rather than between the intracellular and extracellular milieu. These channels are called gap junction channels, an expression which dates back to their ultrastructural detection by Revel and Karnovsky (1967) who

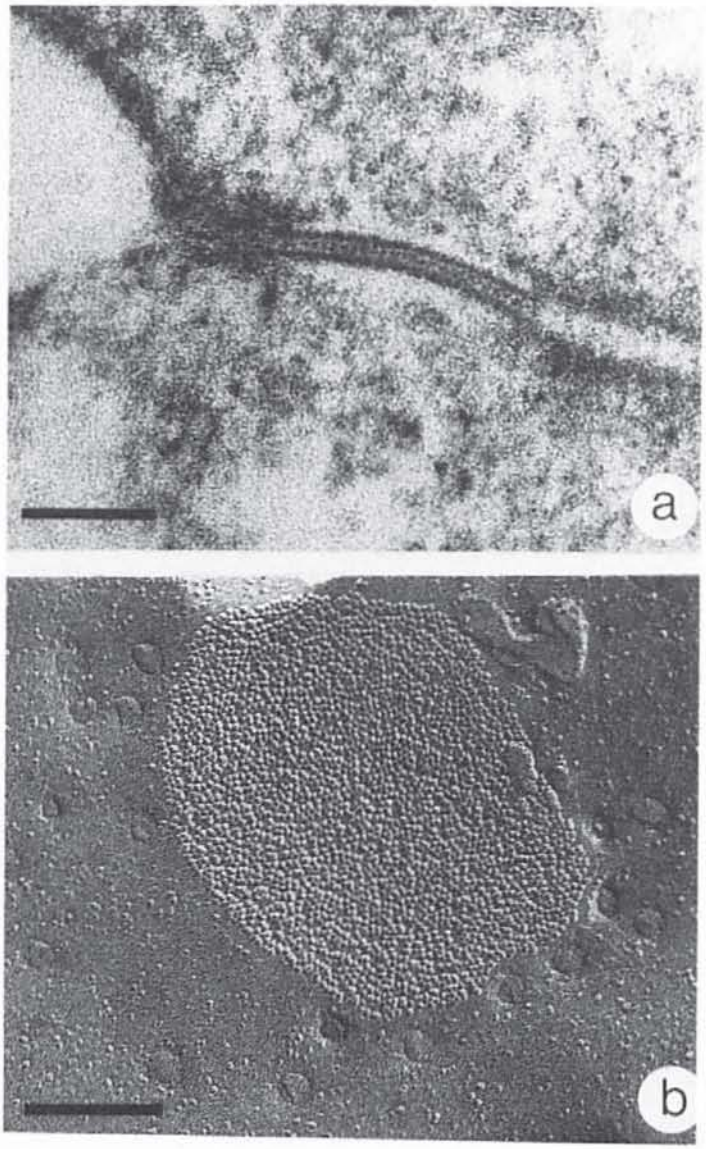

Fig. 11: a. Electron micrograph of a thin section of a gap junction between mammary tumor cells of the Marshall rat (BICR/M1R$_K$). Note the dark stained "gap" between the apposed membranes, from which the name gap junction is derived (bar: 100 nm).
b. Freeze fracture replica of a gap junction plaque in murine glia cells (bar: 200 nm).

described structures which were characterized by a hexagonal array and a 3 nm gap between the membranes of adjacent cells (Fig. 11a). Many gap junction channels are aggregated to gap junctional plaques which are easily recognized in freeze fracture preparations (Fig. 11b).Gap junctions are associated with intercellular communication, they are already present in the very early development of embryos, long before humoral or neuronal communication

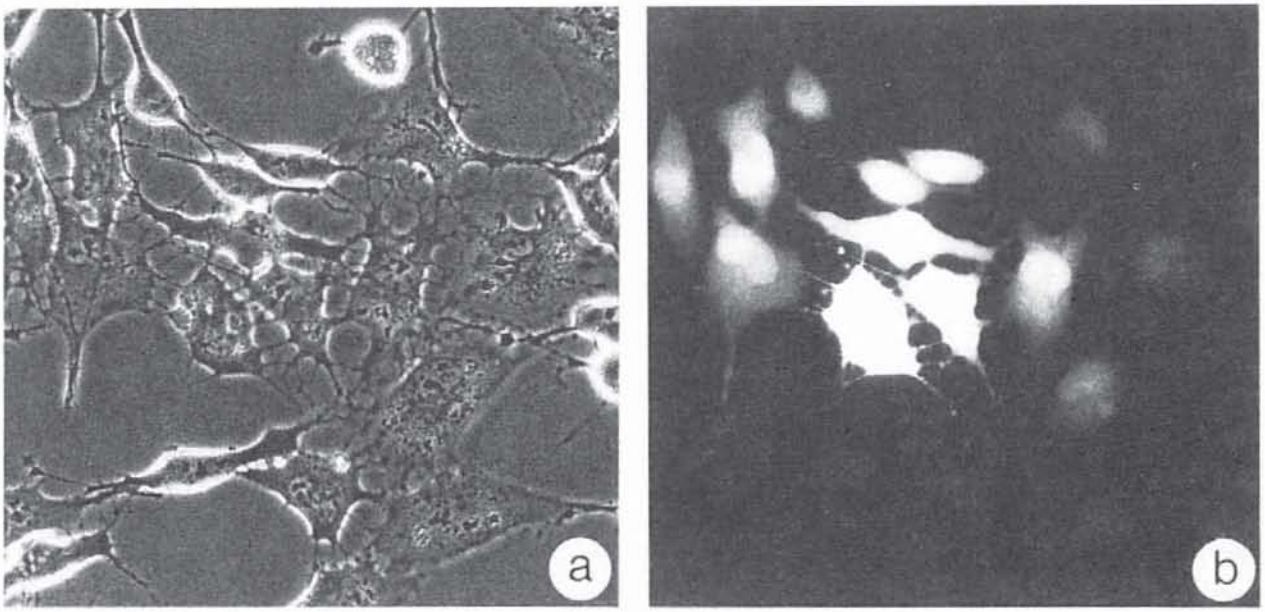

Fig. 12: Demonstration of intercellular communication in mammary tumor cells of the rat (BICR/M1R$_K$). The fluorescent dye Lucifer Yellow spreads via gap junctions from one cell into its neighbours. The dye was iontophoretically injected into one cell and spreading was monitored under an epifluorescence microscope.
a. Phase contrast picture of BICR/M1R$_K$ cells.
b. Fluorescence picture of the same cells.

is established (Warner, 1988). It has been shown (Flagg-Newton et al., 1977) that besides the transfer of small ions (e.g. K^+), a variety of molecules up to 900 Dalton may pass through gap junction channels of mammalian cells (cf. Fig. 12). Cells that are "coupled" to each other via gap junctions, therefore, may be considered as an electric and metabolic syncytium for most metabolites and second messenger molecules. Though much is known about structure and function of gap junctions (Unwin & Zampighi, 1980; Pitts & Finbow, 1986), only very few data are available about the gating mechanisms of these channel forming molecules (e.g. Neyton & Trautman, 1985; Veenstra & DeHaan, 1986).
The problems of double whole cell recording experiments become evident when one studies the equivalence circuit of the setup (Fig. 13). A current can only flow through gap junction channels when a transjunctional potential difference is maintained between the cytoplasm of two cells. Experimentally this is achieved by clamping cell A to a fixed transmembrane potential while cell B is kept at its resting potential. If the two potentials differ from each other, there will also be a potential difference across the gap junction which generates a current through gap junction channels. Every change in the amplitude of this current, which can be measured in both cells, must be attributed to an opening or closing of these gap junction channels. It is noteworthy, however, that the membrane resistance of the cell also contributes to the total noise in the record. This is most evident for cell A, when its transmembrane potential is clamped to values differing considerably from its resting potential. The signal to noise ratio may be improved to values where single channel events become visible by low pass filtering with low cut-off frequencies, which - on the other hand -

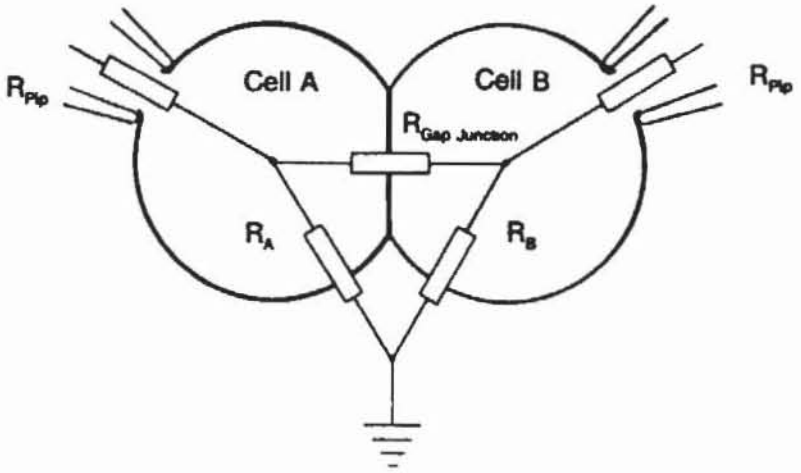

Fig. 13: Equivalent circuit for double whole cell recording.
R_{Pip} = pipette resistance
$R_{Gap\ Junction}$ = resistance of the gap junction
R_A = membrane resistance of cell A
R_B = membrane resistance of cell B

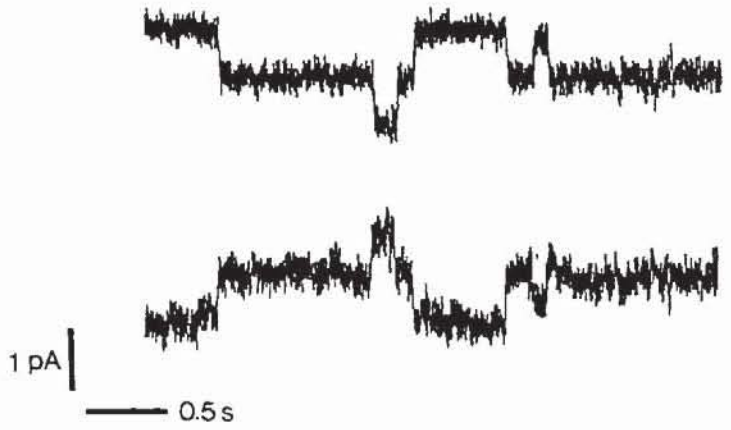

Fig. 14: Current recordings from double whole cell recordings with freshly isolated pairs of PLC cells, a permanently growing human hepatoma cell line. Lower trace is from cell A (the clamped cell), upper trace from cell B (resting cell). Note the reduced background noise level in the resting cell.

reduces the time resolution of these records considerably. Double whole cell recordings are, therefore, preferentially performed with small cells which are characterized by high input resistances and low internal membrane noise. The experiments demonstrated in Fig. 14 have been performed with freshly prepared PLC cell pairs and low pass filtering was applied at corner frequencies of 250 to 500 Hz (eight pole Bessel filter, Type 902 LPF, Frequency Devices Inc., Haverhill MA, USA) which reduced the effective time resolution towards 4 to 8 ms.

Data analysis

A look at a single channel record (Fig. 15) reveals two properties which can be analyzed: the current amplitude and the durations of open and closed states. Accordingly two different models for the behaviour of membrane channels are discussed. A static model describes the electrical properties of ion channels and relates them to structural features (Hille, 1984). The dynamic behaviour is related to chemical kinetics and, therefore, links the functional aspects of channels with physiological properties of the cell (DeFelice & Clay, 1983; Lecar, 1986; Moczydlowski, 1986).

Current amplitudes are usually distributed with two or more predominant levels. The steps between two levels are of quantal nature, therefore, the levels are commonly interpreted as open or closed states of a pore with a fixed diameter (Hille, 1984). This can be seen in Fig. 16, which is the current amplitude distribution of the single channel record shown in Fig. 15. The Gaussian distribution of the current amplitudes is due to superpositions of the channel current signals with noise signals from the amplifier and the membrane. Transitions between states are faster than the time resolution of the recording system, giving rise to the

rectangular appearance of the fluctuations. This fast transition points to a gating mechanism which is due to a minute charge movement rather than a global conformational change of the channel forming molecules. The amplitude of the fully open state of a channel is called its unit current. From this unit current and the applied holding potential the unit

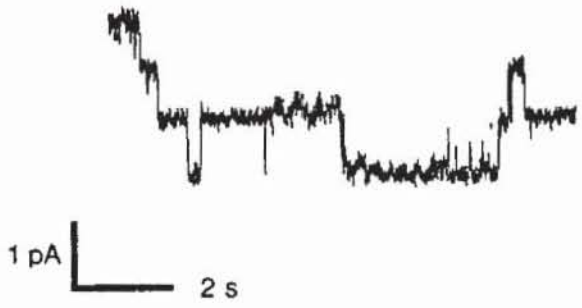

Fig. 15: Single channel record from gap junction channels in PLC cell pairs.

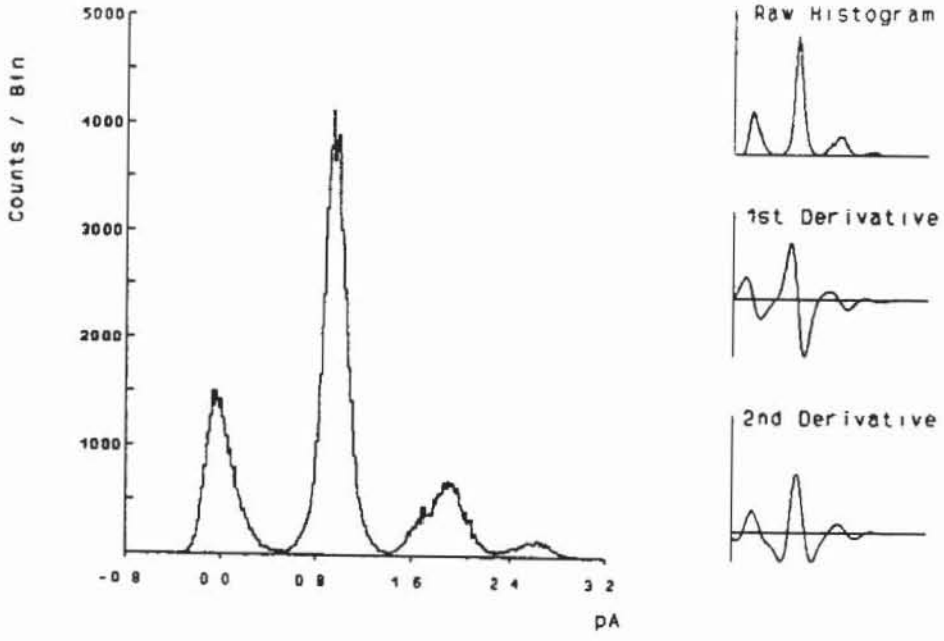

Fig. 16: Amplitude histogram from the record in Fig. 15.

conductance of the channel may be computed. Usually this is derived from the slope of the current to voltage relationship determined for this channel. This is shown in Fig. 17 for the two main conductance states of gap junction channels in PLC cells.
The unit conductance is a characteristic specification for a channel species, a second characteristic is indicated by the intersect of the I/U curve with the voltage axis, the reversal potential U_{rev}. The reversal potential is defined as the voltage offset at zero current and is given by the Goldmann equation as:

$$U_{rev} = \frac{RT}{zF} \cdot \ln \frac{[M]_o + \kappa[A]_i}{[M]_i + \kappa[A]_o} \qquad (1)$$

with

$$\kappa = \frac{P_A}{P_M}$$

where κ is the relative permeability of anions (A) with regard to cations (M). By determining the permeability ratios of different ion pairs from their reversal potentials, the ion selectivity of the channel can be derived.
For some channels ultrastructural information is available and may be correlated to electrical properties of corresponding single channel records. For example, from electron microscopical pictures and X-ray diffraction analysis of the gap junction channel, Makowski et al. (1977) computed an estimate for its inner diameter of 1 - 1.5 nm, its outer diameter

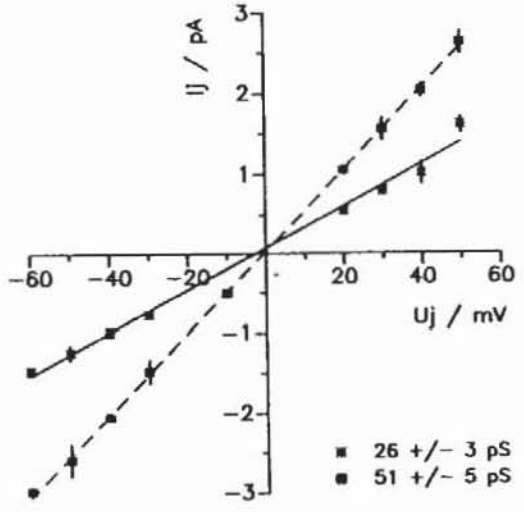

Fig. 17: Current to voltage relationship for the two most frequent conductance steps of gap junction channels in isolated PLC cell pairs. In this case the reversal potential is zero because of the symmetric ion distribution in both cells and the unspecificity of gap junction channels to most smaller ions.
Ij = transjunctional current Uj = transjunctional voltage

of about 6.5 nm, and its pore length of about 15 nm and proposed a structural model as is shown in Fig. 18. This ultrastructural model matches the equivalent circuit depicted in Fig. 19. The gating mechanism of the channel corresponds to a switch between the open channel resistance R_{Ch} and the membrane resistance R_{Mem} in the equivalent circuit. The ion selectivity, probably a result of the electric field in the inner pore, is depicted as a voltage source which is directly equivalent to the reversal potential. From Ohm's law the open channel resistance for this model circuit is given as:

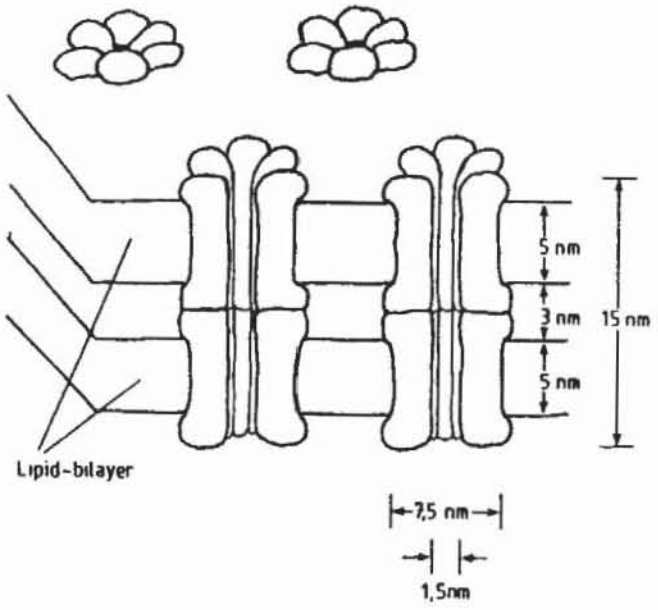

Fig. 18: Structural model for the gap junction channel (redrawn from Makowski et al. 1977)

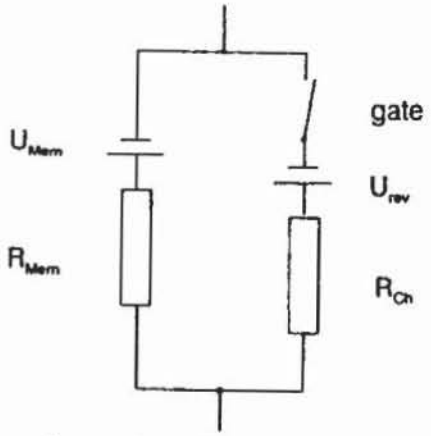

Fig. 19: Equivalence circuit for a membrane channel.
R_{Mem} = membrane resistance R_{Ch} = open channel resistance
U_{Mem} = membrane potential U_{rev} = reversal potential

$$R_{Ch} = \frac{dU}{dI} = constant \tag{2}$$

According to Hille (1984) this can be related to channel geometry via the following relation:

$$R_{Ch} = R_{access} + R_{pore} \tag{3}$$

I.e. the channel open resistance is a combination of the resistance of the channel pore (considered to be cylindrical) in series to an access resistance for ions passing from the bulk solution of the cytosol into the pore mouth. Both terms may be written as

$$R_{pore} = \frac{\rho l}{\pi r^2} \quad and \quad R_{access} = \frac{\rho}{2r} \tag{4}$$

Here stands for the resistivity of the cytosol, r for the effective channel radius, and l for the pore length. Assuming a cytoplasmic resistivity of about 0.64 Ωm (Frank & Hülser, unpublished data) a maximal conductance ranging from 77 to 170 pS can be predicted for gap junction channels which fits well to the values observed from single channel records of BRL and FL (60 and 95 pS) and PLC cell pairs (26 and 51 pS), respectively (Paschke, 1989). A more detailed discussion of pore theory is found in Hille (1984).
Opening and closing of membrane channels are a random process which is related to common chemical kinetics by the theory of stochastic processes (Colquhoun & Hawkes, 1977; 1981; 1982; 1983). In brief, the opening and closing of membrane channels may be expressed according to the following simplified scheme

$$open \underset{\beta}{\overset{\alpha}{\rightleftharpoons}} closed \tag{5}$$

i.e. a chemical equilibrium between the open and closed conformation of the channel, where α and ß are the rate constants of the opening and closing reaction, respectively. In single channel records it is possible to discriminate between these two components, thus

$$open \overset{\alpha}{\rightarrow} closed \tag{6}$$

However, since we are looking at a single molecule, α may no longer be interpreted as a rate constant but rather as a transition probability from the open to the closed state (Colquhoun & Hawkes, 1983). Then the conditional probability of a closing within the short time interval Δt is given by the term

$$P_{(o \to dc)} = \alpha \Delta t + o(\Delta t) \tag{7}$$

If the system is in thermodynamic equilibrium this reaction may be described in terms of Markov processes, where the following differential equation holds (Cox & Miller, 1980; Colquhoun & Hawkes, 1983)

$$\frac{dP(t)}{dt} = -\alpha P(t) \qquad (\alpha - const) \tag{8}$$

where P(t) stands for the probability of an open time τ with a duration of at least t. From this the probability density function $f(\tau)$ of the open lifetimes can be derived which are of the form of an exponential distribution (Cox & Miller, 1980)

$$f(\tau) = \alpha e^{-\alpha \tau} \tag{9}$$

with a mean open time

$$\tau_{mean} = 1/\alpha \tag{10}$$

In fact, histograms of open or closed times from single channel records follow an exponential decay function as is demonstrated in Fig. 20 for gap junction channels. However, the kinetic model shown so far is an oversimplification since true channels usually express a more complex behaviour. There are often two or more kinetic states which correspond to conformations with equal conductivity. On current recordings they are not distinguishable, the analysis of lifetimes, however, helps to discriminate different kinetic states (Fredkin et al., 1985). In these cases, the lifetimes are no longer distributed according to a simple exponential decay function. For lumped systems with n (experimentally undistinguishable) states the lifetime distribution can be expressed as a sum over n exponential terms

$$f(\tau) = \sum_{n} \omega_n e^{-\alpha_n \tau} \tag{11}$$

This is also true for the gap junction channels as can be assumed from Fig. 20. An exact analysis for this special type of channels, however, is hindered because gap junction channels are somehow aggregated and so far no information is available about possible cooperative effects between the individual channels. In addition, the insufficient time resolution of our records allows no detection of events with a duration less than about 1 ms.

Patch clamp data can be related to physiological functions

The voltage gated sodium channel in the axonal membrane of nerve fibers mediates the sodium currents which occur when an action potential is triggered, a property of excitable membranes which has already been analyzed by Hodgkin et al. (1952). To explain the molecular behaviour of this channel species a minimum kinetic model with three states is required (Aldrich & Yellen, 1983)

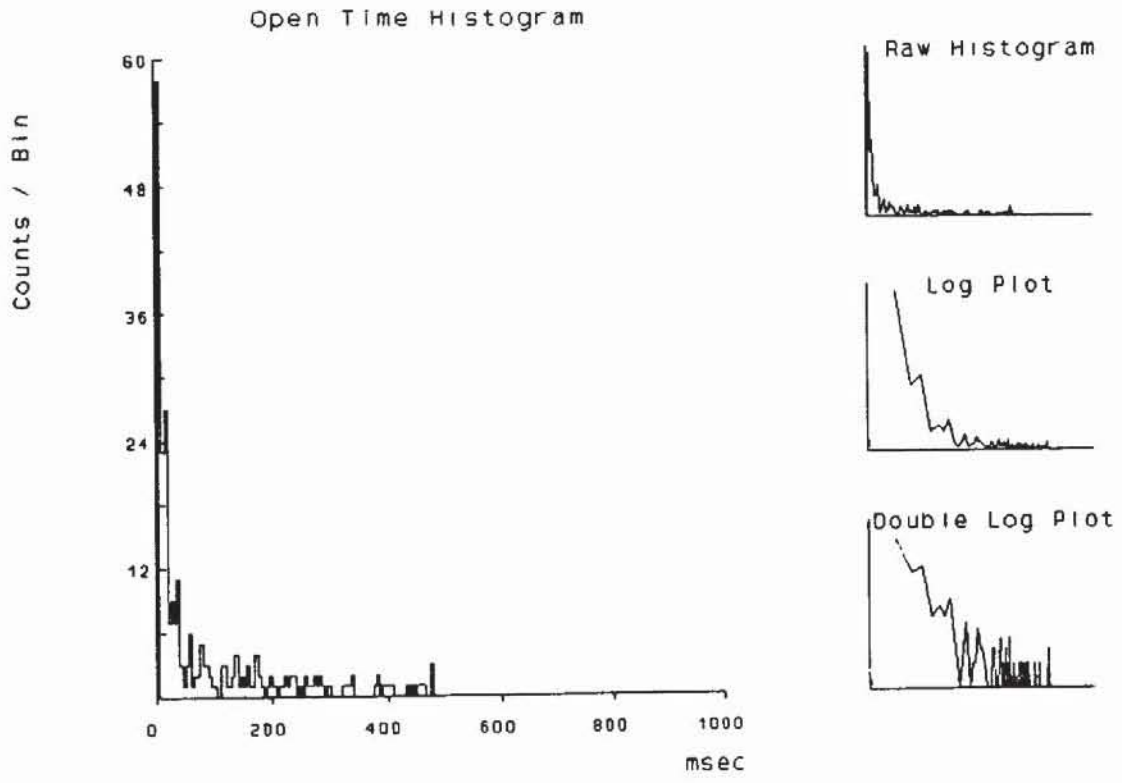

Fig. 20: Open time histogram for gap junction channels in PLC cells.

$$closed \underset{\beta}{\overset{\alpha}{\rightleftharpoons}} open \underset{\delta}{\overset{\gamma}{\rightleftharpoons}} inactivated$$

In this model the closed and inactivated conformation share the same (zero) conductance. The rate constant α is a function of the transmembrane potential. When the transmembrane potential is more negative than the threshold potential, the opening rate constant α is small compared with ß, the rate constant of its backward reaction. Under these conditions most of the channels remain in the closed state. This changes rapidly after a threshold voltage is crossed towards more positive transmembrane potentials. Now α increases, resulting in a considerably higher open probability of the sodium channels which accounts for the fast sodium influx at the beginning of the action potential. From the open state the channel may eventually emerge to the inactivated state where it will stay for a long time period because the time constant δ of the backward reaction is small (some ms). This accounts for the refractory period at the end of an action potential. In single channel recordings such kinetic schemes may directly be recognized if the rate constants ß and δ (or α and $\not\alpha$) are significantly different. In this case openings (or closings) tend to occur in "bursts", a rapid succession of openings (closings) separated by long periods, where the channel is inactive. Bursting behaviour is also seen in transmitter activated channels, e.g. the acetylcholine (Colquhoun & Sakmann, 1983) or the glutamate receptor (Cull-Candy & Parker, 1983) which mediate postsynaptical potentials. Here the "inactivation" of the channel is related to the desensitization behaviour of chemical synapses after prolonged agonist exposure.
These examples demonstrate that by means of high resolution patch clamp recordings, physiological properties of the cell membrane may be elucidated on the molecular level of individual ion channels.

References

Aldrich, R.W. and Yellen, G. (1983) Analysis of nonstationary channel kinetics. In: Single Channel Recording (B. Sakmann and E. Neher eds.), Plenum Press, New York, pp 287-299

Bezanilla, F. (1985) A high capacity data recording device based on a digital audio processor and a video cassette recorder. Biophys. J. 47 : 437-441

Bräuner, T. (1987) Interzelluläre Kommunikation und invasives Wachstum maligner Zellen. Stöffler & Schütz, Stuttgart.

Burt, J.M. and Spray, D.C. (1988) Single channel events and gating behavior of the cardiac gap junction channel. Proc. Natl. Acad. Sci. USA 85 : 3431-3434

Camardo, J.S. and Siegelbaum, S.A. (1983) Single-channel analysis in Aplysia neurones: A specific K^+ channel is modulated by serotonin and cyclic AMP. In: Single Channel Recording (B. Sakmann and E. Neher eds.), Plenum Press, New York, pp 409-423

Colquhoun, D. and Hawkes, A.G. (1977) Relaxations and fluctuations of membrane currents that flow through drug-operated channels. Proc. R. Soc. Lond. B 199 : 231-262

Colquhoun, D. and Hawkes, A.G. (1981) On the stochastic properties of single ion channels. Proc. R. Soc. Lond. B 211 : 205-235

Colquhoun, D. and Hawkes, A.G. (1982) On the stochastic properties of bursts of single ion channel openings and of clusters of bursts. Phil.Trans. R. Soc. Lond. B 300 : 1-59

Colquhoun, D. and Hawkes, A.G. (1983) The principles of the statistical analysis of single channel records. In: Single Channel Recording (B. Sakmann and E. Neher eds.), Plenum Press, New York, pp 135-174

Colquhoun, D. and Sakman, B. (1983) Bursts of openings in transmitter-activated ion channels. In: Single Channel Recording (B. Sakmann and E. Neher eds.), Plenum Press, New York, pp 345-364

Corey, D.P. and Stevens, C.F. (1983) Science and technology of patch-recording electrodes. In: Single Channel Recording (B. Sakmann and E. Neher eds.), Plenum Press, New York, pp 53-68

Cota G. and Armstrong C.M. (1984) Potassium channel "inactivation" induced by soft-glass patch pipettes. Biophys. J. 53 : 107-109

Cox, D.R. and Miller, H.D. (1980) The theory of stochastic processes. Chapman and Hall, London

Cull-Candy, S.G. and Parker, I. (1983) Experimental approaches used to examine single glutamate-receptor ion channels in locust muscle fibers. In: Single Channel Recording (B. Sakmann and E. Neher eds.), Plenum Press, New York, pp 389-400

DeFelice, L.J. and Clay, J.R. (1983) Membrane current and membrane potential from single-channel kinetics. In: Single Channel Recording (B. Sakmann and E. Neher eds.), Plenum Press, New York, pp 323-342

Flagg-Newton, J., Simpson, I. and Loewenstein, W.R. (1979) Permeability of the cell-to-cell membrane channels in mammalian cell junction. Science 205 : 404-407

Fredkin, D.R., Montal, M. and Rice, J.A. (1985) Identification of aggregated markovian models : Application to the nicotinic acetylcholine receptor. In: Proceedings of the Berkeley Conference in Honor of Jerzy Neyman and Jack Kiefer Vol. 2 (L.M. LeCam and R.A. Olsen eds.), Wadsworth Publishing, Belmont CA, pp 269-289

Hamill, O.P., Marty, A., Neher, E., Sakmann, B. and Sigworth, F.J. (1981) Improved patch-clamp techniques for high-resolution current recording from cells and cell-free membrane patches. Pflügers Arch. 391 : 84-100

Hille, B. (1984) Ionic channels of excitable membranes. Sinauer Associates, Sunderland MA.

Hodgkin, A.L., Huxley, A.F. and Katz, B. (1952) Measurement of current-voltage relations in the membrane of the giant axon of Loligo. J. Physiol. 116 : 424-448.

Horn, R. and Marty, A. (1988) Muscarinic activation of ionic currents measured by a new whole-cell recording method. J. Gen. Phys. 92 : 145-159

Kostyuk, P.G., Krishtal, O.A. and Pidoplichko, V.I. (1981) Intracellular perfusion. J. Neurosci. Meth. 4 : 201-210

Lapointe, J.-Y. and Szabo, G. (1987) A novel holder allowing internal perfusion of patch-clamp pipettes. Pflügers Arch. 410 : 212-216

Lecar, H. (1986) Single-channel currents and postsynaptic drug actions. In: Ionic Channels in Cells and Model Systems (R. Latorre ed.), Plenum Press, New York, pp 17-36

Marty, A. and Neher, E. (1983) Tight-seal whole-cell recording. In: Single Channel Recording (B. Sakmann and E. Neher eds.), Plenum Press, New York, pp 107-122

Makowski, L., Caspar, D.L.D., Philips, W.C. and Goodenough, D.A. (1977) Gap junction structures. II. Analysis of the X-ray diffraction data. J. Cell Biol. 74 : 692-645

McCann, F.V., Stibitz, G.R. and Keller, T.M. (1987) A computer method for the acquisition and analysis of patch-clamp single-channel currents.
J. Neurosci. Meth. 20 : 45-55

Moczydlowski, E. (1986) Single channel enzymology. In: Ion Channel Reconstitution (C. Miller ed.), Plenum Press, New York, pp 75-113

Neher, E. and Sakmann, B. (1976) Single channel currents recorded from membranes of denervated frog muscle fibers. Nature 260 : 799-802

Neyton, J. and Trautman, A. (1985) Single-channel currents of an intercellular junction. Nature 317 : 331-335

Paschke, D. (1989) Gap-Junction-Kanäle mit unterschiedlichen Leitfähigkeiten. Dissertation, Universität Stuttgart

Pitts J.D. and Finbow, M.E. (1986) The gap junction. J. Cell Sci. Suppl. 4 : 239-266

Pusch, M. and Neher, E. (1988) Rates of diffusional exchanges between small cells and a measuring patch pipette. Pflügers Arch. 411 : 204-211

Rae, J.L. and Lewis, R.A. (1984) Patch clamp recordings from the epithelium of the lens obtained using glass selected for low noise and improved sealing properties. Biophys. J. 45 : 144-146

Revel, J.-P. and Karnovsky, M.J. (1967) Hexagonal array of the subunits in intercellular junctions of the mouse heart and liver. J. Cell Biol. 33 : C7-C12

Sakmann, B. and Neher, E. (1983) Geometric parameters of pipettes and membrane patches. In: Single Channel Recording (B. Sakmann and E. Neher eds.), Plenum Press, New York, pp 37-51

Sigworth, F.J. (1983) Electronic design of the patch clamp. In: Single Channel Recording (B. Sakmann and E. Neher eds.), Plenum Press, New York, pp 3-35

Somogyi, R. and Kolb, H.-A. (1988) Cell-to-cell channel conductance during loss of gap junctional coupling in pairs of pancreatic acinar and Chinese hamster ovary cells. Pflügers Arch. 412 : 54-65

Unwin, P.N.T. and Zampighi, G. (1989) Structure of the junctions between communicating cells. Nature 283 : 545-549

Veenstra, R.D. and DeHaan, R.L. (1986) Measurement of single channel currents from cardiac gap junctions. Science 233 : 972-974

Warner, A. (1988) The gap junction. J. Cell. Sci. 89 : 1-7